

Investigating individual chromophores within single porous silicon nanoparticles

M. D. Mason, D. J. Sirbuly, P. J. Carson, and S. K. Buratto^{a)}

Department of Chemistry and Biochemistry, University of California at Santa Barbara, Santa Barbara, California 93106-9510

(Received 3 November 2000; accepted 24 January 2001)

We use single nanoparticle luminescence microscopy to determine a distribution of individual chromophores present in porous Si nanoparticles. From these distributions, we determine the average number of emitting chromophores in each nanoparticle and the fluorescence emission count rate of a single chromophore within the porous silicon nanoparticle. We also show that the same size nanoparticles prepared under two different electrochemical conditions have different fluorescence peak maxima, and exhibit different chromophore number distributions, consistent with the quantum confinement model for the luminescence in porous silicon. © 2001 American Institute of Physics.

[DOI: 10.1063/1.1355764]

INTRODUCTION

Visible light emission from Si via anodic etching in aqueous HF (called porous Si) has stimulated tremendous interest over the past several years due to its potential application in optoelectronic devices such as light emitting diodes and lasers and the ability to be integrated with current Si processing technology.^{1,2} The visible photoluminescence in porous silicon has been attributed primarily to a confinement effect, determined by the Si grain size.³

Although a quantum confinement model for the emission mechanism of as-prepared porous silicon has gained widespread support, the high degree of structural inhomogeneity and parametric tunability of etched bulk samples have made a direct correlation between chromophore size and optical band gap difficult.⁴ General support for a quantum confinement model is drawn from a host of fluorescence data, including a dramatic shift toward higher emission energies with an increase in the bulk porosity, which presumably results in a decrease in the Si grain size.⁵ However, due to the structural inhomogeneity of the Si framework within the bulk porous silicon structure, a direct correlation between the Si grain size and the observed shift in band gap has been elusive. In order to investigate this relationship in detail, recent studies from our group have focused on removing the Si chromophore from the bulk and applying single molecule spectroscopic techniques.⁶⁻⁸

Our previous experiments have shown that colloidal porous Si samples can be dispersed on a glass cover slip such that the average distance between nanoparticles is $>0.5 \mu\text{m}$. The emission properties of the individual nanoparticles are then probed in the absence of spatial averaging. These initial single nanoparticle luminescence experiments uncovered a number of new phenomena in porous Si such as resolved vibronic structure in the emission spectrum, luminescence intermittency, random spectral wandering, and coupling between adjacent chromophores. The main conclusion drawn

from these data was the strong influence of the surface and the surface-passivating layer on the emission from the porous Si nanoparticles. Our results suggest that the emission from porous Si nanoparticles originates from excitons in a quantum confined crystalline Si core, strongly coupled to the surface of the quantum dot, which is a relatively thick matrix of siloxene (SiO_xH_y) species. Further work from our group has demonstrated that, on average, fewer than 3% of nanoparticles prepared from bulk porous silicon are luminescent,⁹ which is consistent with the relatively low quantum efficiency of bulk porous silicon (1%–5%).¹⁰⁻¹³ Taking this into account it is possible that the emission properties of a single particle is strongly dependent on the structure of the surface and the relationship between the number and size of the chromophores (crystalline regions) present in the nanoparticle.

In order to examine the relationship between the Si chromophore and the nanoparticle more closely we employ several spectroscopy and microscopy techniques including: (1) fluorescence microscopy, (2) single-particle spectroscopy, and (3) shear-force microscopy on a series of size-selected, surface-modified single nanocrystals. We apply simple statistical techniques to provide a more complete picture of the electronic structure of the luminescent species within these nanoparticle systems.

EXPERIMENT

Colloidal porous Si samples were prepared from bulk porous Si using the method of Heinrich *et al.* In these experiments, *p*-type Si was anodically etched in a 1:1:1 by volume solution of hydrofluoric acid (49%), ethanol, and hydrogen peroxide (30%). Red and green emitting porous silicon bulk samples were prepared by electrochemically etching for 20 minutes at 5 mA/cm^2 [low current density (LCD)], or 10 min at 10 mA/cm^2 [high current density (HCD)], respectively. The total number of silicon atoms removed is equivalent to the half the number of injected charges (holes),⁴ which is simply the current density multiplied by

^{a)}Electronic mail: buratto@chem.ucsb.edu

the etch time. In each case discussed here the same quantity (3.0×10^{-5} mol) of silicon atoms was removed. The resulting bulk morphologies, however, are dramatically different owing to a larger pore volume, and a decrease in the size of the silicon framework, as the current density is increased.¹⁴ The resulting porous silicon layer was mechanically removed from the surface and sonicated for 24 h in hexanes to reduce particle size. The larger particles were allowed to settle out of solution and the top portion of the solvent containing only the smallest nanoparticles was removed. Samples of spatially separated porous Si nanoparticles were prepared by diluting this stock solution (~ 1 nM) and spin casting a $30 \mu\text{L}$ aliquot of the diluted solution onto a clean glass coverslip.

Emission from single nanoparticles was imaged in the far field using a laser scanning confocal microscope with a high numerical aperture oil-immersion objective (Zeiss, 1.3 NA) described in detail in a previous publication.⁸ For all experiments, the 457 nm line of an Ar^+ laser (Spectra-Physics) was used as the excitation source. The diffraction-limited excitation spot was focused on the sample side opposite the immersion oil. Using a beam-splitter in the path of the collected fluorescence signal, we were able to acquire emission intensity images (Digital Instruments) and emission spectra (Princeton Applied Research) simultaneously.

Shear force microscopy⁶ was used to determine the surface topography of the nanoparticles on glass. In this technique (an analog of attractive mode atomic force microscopy) a pulled tapered fiber-optic tip is attached to a small piezoelectric tube and dithered on its mechanical resonance. The tip-sample distance is determined by monitoring the dither amplitude as the sample approaches the tip. The dither amplitude is measured by focusing laser light on the probe tip and monitoring the scattered light synchronously with the dither frequency using a lock-in amplifier. This amplitude provides input for the feedback loop of our scanning electronics, which are set to maintain a constant height above the sample surface (approximately 10 nm). A topography image is then acquired by digitizing the output of the feedback loop. It is important to note that the size of the tip is ~ 100 nm, which is the limit of the lateral resolution. The height, however, is measured with a resolution of a few angstroms, the noise on our feedback signal.

RESULTS AND DISCUSSION

The fluorescence image shown in Fig. 1 is a typical confocal image ($15 \times 15 \mu\text{m}^2$) of one of our samples dispersed on glass. Each 250 nm bright spot indicates a luminescing nanoparticle. It is important to note that the size of bright spot represents the diffraction limited size of the illumination spot and not the size of the nanoparticle. The distance between adjacent nanoparticles is at least $1 \mu\text{m}$ ensuring adequate isolation.

The emission spectra shown in Fig. 2 are for two porous Si nanoparticle samples prepared under different electrochemical conditions. The spectrum shown in Fig. 2(a) is for a sample etched at 10 mA/cm^2 for 10 min (HCD sample) Fig. 2(a), and the spectrum in Fig. 2(b) was prepared by etching at 5 mA/cm^2 for 20 min. Each spectrum was obtained by integrating over several scan lines in the fluores-

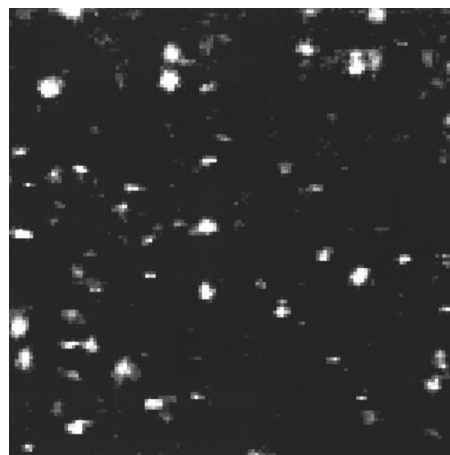


FIG. 1. Representative fluorescence (LCSM) image of single nanoparticles deposited on glass. The bright spots represent spatially isolated nanoparticles on a linear gray scale (white ~ 20 kcps). The image size is $15 \mu\text{m} \times 15 \mu\text{m}$.

cence image (Fig. 1), and represents the average of ~ 10 nanoparticles. Nanoparticles prepared under LCD conditions (gray line) show strong red luminescence with a maximum at 675 nm. Those prepared using HCD conditions (black line) exhibit a slightly broadened spectrum which is blueshifted and has a maximum at 550 nm. In both cases the spectral peak maximum of the original bulk is conserved when converted into a nanoparticulate colloid. Furthermore, while both sample types have broad spectra at room temperature, the relative asymmetry of the HCD line shape suggests that the distribution of chromophore sizes in each sample is different.

Evidence for multiple chromophores is also observed in the emission from individual nanoparticles. The line trace of Fig. 3 shows the fluorescence intensity of an individual nanoparticle as a function of time. The intensity trajectory (time course) shown in Fig. 3 was acquired for a single LCD nanoparticle under $5 \mu\text{W}$ of cw 457 nm excitation and is

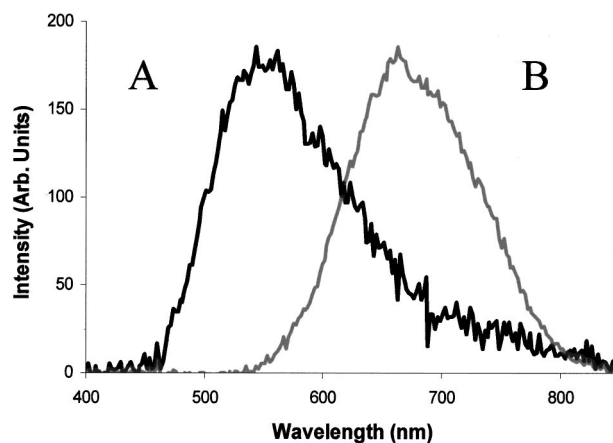


FIG. 2. Photoluminescence spectra of porous silicon nanoparticles dispersed on glass. Each spectrum shown is the average of ~ 10 single particle spectra (10 s integration time), under 488 nm cw excitation. Nanoparticles prepared using low current density (gray line) exhibit a characteristic fluorescence maximum ($\lambda_{\text{max}} = 675$ nm) significantly redshifted from high current density samples (black line) ($\lambda_{\text{max}} = 550$ nm).

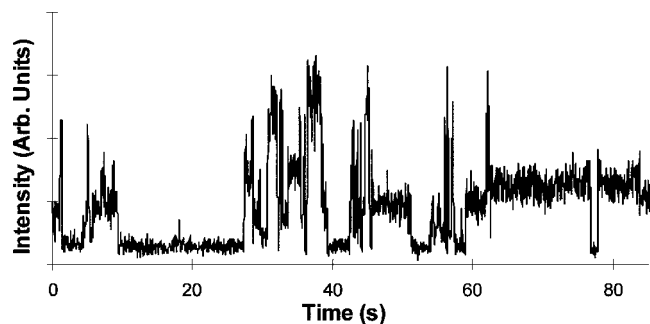


FIG. 3. Intensity trajectory (time course) of a single low current density porous silicon nanoparticle dispersed on glass. The data shown were acquired with 125 ms bin times, and additionally binned by 8 to emphasize the apparent multilevel blinking behavior.

representative of both the HCD and LCD samples. The rapid jumps in intensity, referred to as “blinking,” are the result of an Auger type ionization mechanism and are described in detail elsewhere.^{8,15} Of particular interest is the apparent multilevel structure, which in single molecule spectroscopy is often attributed to a system having several emitting species.¹⁶

In order to investigate the individual chromophore(s) within the silicon nanoparticle it is necessary to first examine the relationship between the nanoparticle size and the size of the quantum confined silicon chromophore. The image shown in Fig. 4(a) is a representative shear-force topography image of an $8 \times 8 \mu\text{m}$ area of a LCD sample. A bright spot in the topography image indicates a nanoparticle. On the height scale shown the blank glass cover slip is nearly flat. As mentioned previously, if the size of the nanoparticle is much smaller than the tip itself, as in this case here, then the nanoparticle images the tip rather than the reverse. As a result all features appear the same size in the lateral dimensions [as seen in Fig. 4(b)]. If we assume as a first-order approximation that each nanoparticle is roughly spherical then the height of each feature in Fig. 4(b) is a more accurate representation of the particle size than the lateral width. We have applied this approach to the LCD and HCD samples and in both cases the average nanoparticle size is approximately 6 nm with 95% of particles falling within the range of 4.5–7 nm. Previous theoretical work has suggested that visible luminescence from a quantum confined grain of silicon will only occur at diameters $<4 \text{ nm}$.¹⁷ Therefore, in light of the quantum confinement model, the silicon chromophore must represent a relatively small volume of the entire nanoparticle. As mentioned earlier, the crystalline silicon framework, and therefore the Si “quantum dot” is expected to be much smaller in the HCD samples, since the emission spectrum is blueshifted relative to the spectrum of the LCD sample (Fig. 2). This also suggests the possibility of multiple chromophores in a single nanoparticle and that there may be more chromophores/nanoparticle in the case of the HCD sample.

In order to investigate the number of chromophores within an individual nanoparticle a statistical method was employed. In this approach, single nanoparticle intensity images were acquired for both the HCD and LCD samples. The fluorescence peaks in the single nanoparticle images exhibit

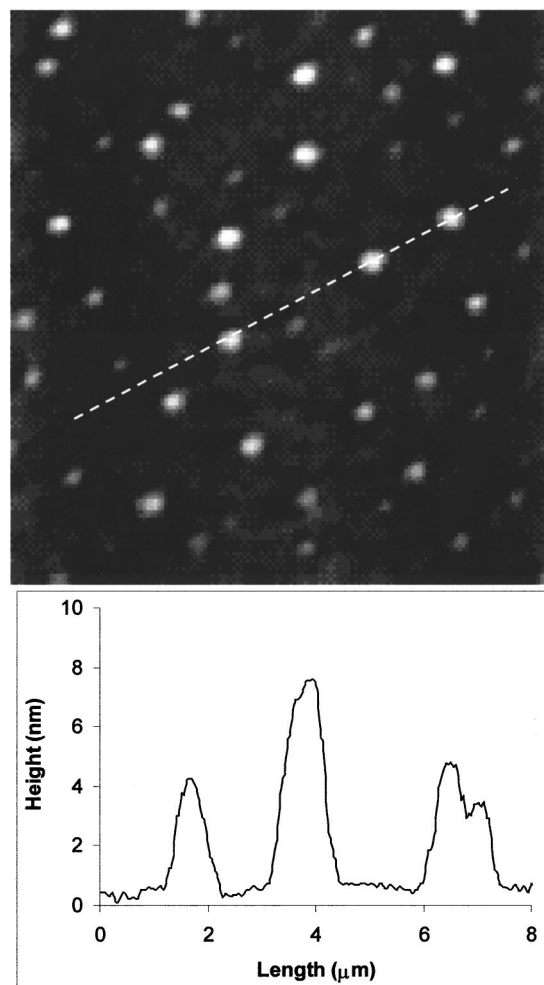


FIG. 4. Shear-force topography image and corresponding line trace for a typical dilute porous silicon nanoparticle sample dispersed on glass. The cross section shown in the line trace was taken along the dashed line shown in the image. The mean nanoparticle height is approximately $\sim 6 \text{ nm}$ with and uncertainty of $<0.5 \text{ nm}$.

a two-dimensional (2D) Gaussian shape [shown in Fig. 5(a)], which is consistent with the intensity profile of diffraction limited excitation area. Each peak in the fluorescence images was fit to a 2D Gaussian and the fit for the data of Fig. 5(a) is presented in Fig. 5(b). The full width at half maximum (FWHM) of all 2D Gaussians and the lateral shape of the 2D Gaussian (circular) were held constant during each fit. The accuracy of each fit was monitored by calculating the 2D residual (data fit), shown in Fig. 5(c), which should result in noise for a good fit (as shown). The peak maxima of each fitted 2D Gaussian were then taken as the fluorescence intensity of each porous silicon nanoparticle.

The single nanoparticle emission intensities were compiled and binned into the histograms shown in Fig. 6 for both LCD and HCD samples [Figs. 6(a) and 6(b), respectively]. The histogram in Fig. 6(a) represents 481 LCD nanoparticles, and the histogram in Fig. 6(b) represents 834 HCD nanoparticles. Each of the histograms shown in Figs. 6(a) and 6(b) has been fitted (heavy black line) to four Gaussians (gray lines). Here, the FWHM of the fitted Gaussians increases as nearly the square root of the peak intensity, which suggests that the fitted parameters are accurately representing

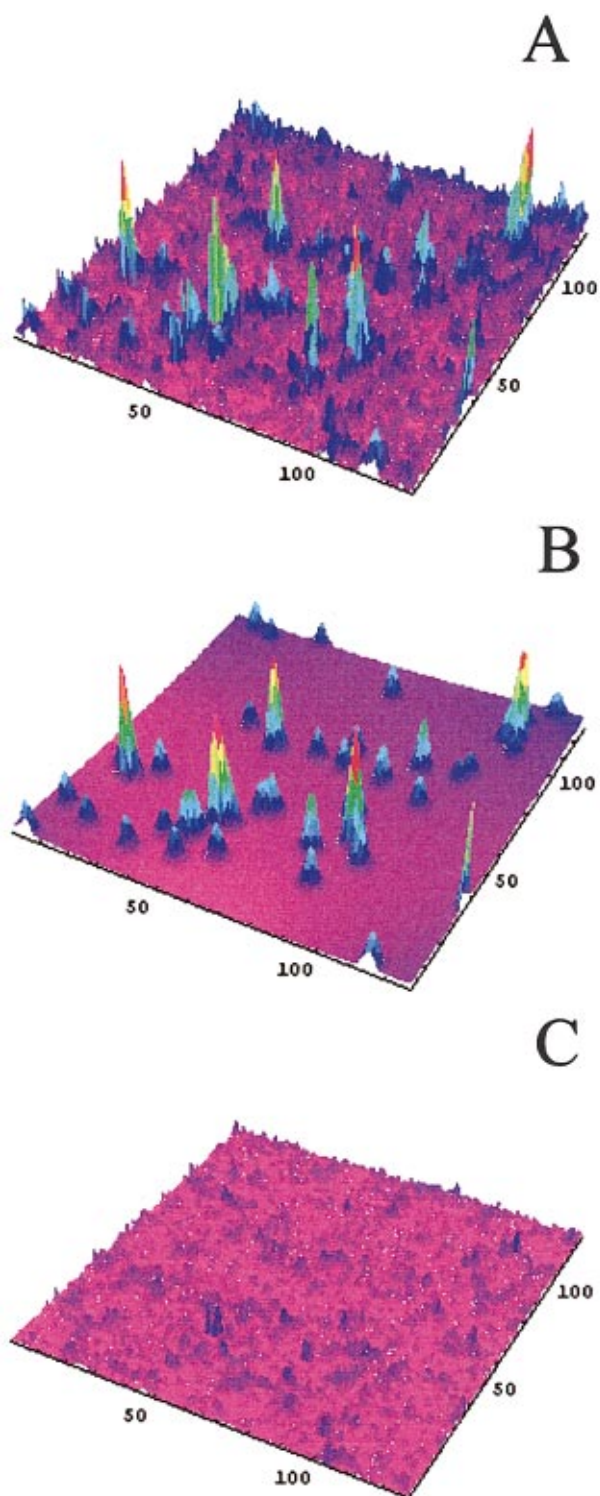


FIG. 5. (Color) Two-dimensional fit to photoluminescence intensity data. (a) Representative $15 \times 15 \mu\text{m}$ raw photoluminescence intensity data, (b) 2D Gaussian fit to data, and (c) fit residual (raw data–simulation).

the ensemble of individual shot noise limited peaks. In all cases, regardless of the number of bins used, the peak position of the first Gaussian was at ~ 2.2 kcps and the mean separation between Gaussians is approximately 2 kcps for both histograms.

If each Gaussian represents a subset of chromophores each emitting with nearly the same intensity, then the posi-

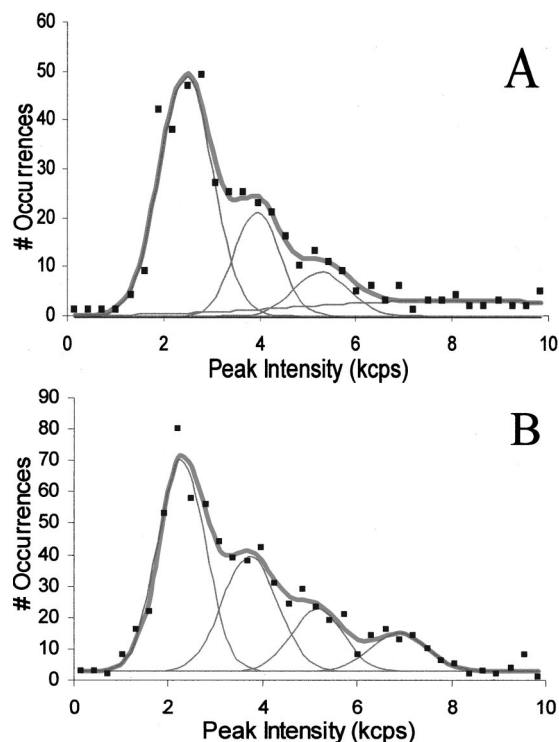


FIG. 6. Intensity histograms and corresponding multiple Gaussian fits of high and low current density porous silicon nanoparticles.

tion of the first peak, and the relative spacing between peaks suggests that the individual chromophore emits with an intensity of ~ 2 kcps (under these excitation conditions). Probably more significant is the overall shape of each histogram which suggests that the average nanoparticle consists of several chromophores. The relative areas of the fitted Gaussians suggest that for the LCD samples [Fig. 6(a)] $\sim 70\%$ of the nanoparticles measured contain only a single emitting chromophore. For the HCD samples, however, fewer than half of the particles measured contain a single emitting chromophore and a significant percentage contain three or four chromophores.

This is consistent with our previous measurements,¹⁴ which show that although HCD prepared samples result in the same size nanoparticles as for the LCD case, they contain less silicon and are therefore more porous. If the individual nanoparticle is simply a small segment of the larger bulk framework, then the HCD nanoparticles should contain smaller crystalline silicon regions. If the nanoparticles measured in the experiments discussed here are the same size and there are, on average, more chromophores in the HCD nanoparticles, then the Si chromophores within the HCD samples must be smaller. From the data discussed here this statement appears to be true. This provides a more direct correlation between the actual Si chromophore size and the position of spectral emission than previous bulk porosity arguments, and is further evidence for the quantum confinement model.

CONCLUSION

Using simple single molecule spectroscopic techniques we have directly probed the optical properties of silicon nanoparticles made from bulk porous silicon. By fracturing

the porous silicon framework into spatially isolated nanoparticles we can remove the effects of spatial averaging while maintaining the optical properties found in the bulk porous silicon framework. We find that nanoparticles prepared under high current density conditions, on average, contain ≤ 4 emitting chromophores, while those prepared under lower current density conditions contain only one or two chromophores that are emitting. Furthermore, our data suggest that the chromophores in the high current density samples must be smaller, and is consistent with the observed spectral blueshift of a confined quantum dot. This work provides a direct link between the number and size of the quantum dots found in porous silicon and their observed photoluminescence emission.

¹L. T. Canham, Appl. Phys. Lett. **57**, 1046 (1990).

²A. G. Cullis, L. T. Canham, and P. D. J. Calcott, Appl. Phys. Lett. **82**, 909 (1997).

³P. M. Fauchet and J. von Behren, Phys. Status Solidi B **204**, R7 (1997).

⁴V. Lehmann and U. Gösele, Appl. Phys. Lett. **58**, 856 (1991).

⁵I. Samuelson, A. Gustafsson, D. Hessman, J. Lindahl, L. Montelius, A. Petersson, and M. E. Pistol, Phys. Status Solidi A **152**, 269 (1995).

⁶E. Betzig, P. L. Finn, and J. S. Weiner, Appl. Phys. Lett. **60**, 2484 (1992).

⁷J. L. Heinrich, C. L. Curtis, G. M. Credo, K. L. Kavanagh, and M. J. Sailor, Science **255**, 66 (1992).

⁸M. D. Mason, G. M. Credo, K. D. Weston, and S. K. Buratto, Phys. Rev. Lett. **80**, 5405 (1998).

⁹G. M. Credo, M. D. Mason, and S. K. Buratto, Appl. Phys. Lett. **74**, 1978 (1999).

¹⁰W. Wilson, P. F. Szajowski, and L. E. Brus, Science **262**, 1242 (1993).

¹¹L. Brus, J. Phys. Chem. **98**, 3575 (1994).

¹²A. L. Efros, M. Rosen, B. Averboukh, D. Kovalev, M. Ben-Chorin, and F. Koch, Phys. Rev. B **56**, 3875 (1997).

¹³F. Muller, R. Herino, M. Ligeon, F. Gaspard, R. Romestain, J. C. Vial, and J. Bsiesy, J. Lumin. **57**, 283 (1997).

¹⁴M. D. Mason, D. J. Sirbuly, P. J. Carson, and S. K. Buratto (unpublished).

¹⁵S. A. Empedocles, D. J. Norris, and M. G. Bawendi, Phys. Rev. Lett. **77**, 3873 (1996).

¹⁶K. D. Weston, P. J. Carson, H. Metiu, and S. K. Buratto, J. Chem. Phys. **109**, 7474 (1998).

¹⁷B. Delley and E. F. Steigmeier, Appl. Phys. Lett. **67**, 2370 (1995).